International Research Journal of Pure & Applied Chemistry

21(3): 37-50, 2020; Article no.IRJPAC.55386
ISSN: 2231-3443, NLM ID: 101647669

Chemical Synthesis of Silver Nanoparticles Using Tri-sodium Citrate, Stability Study and Their Characterization

Prem Santhi Yerragopu[1*], Sharanagouda Hiregoudar[1], Udaykumar Nidoni[1], K. T. Ramappa[1], A. G. Sreenivas[2] and S. R. Doddagoudar[3]

[1]Department of Processing and Food Engineering, College of Agricultural Engineering, University of Agricultural Sciences, Raichur, India.
[2]Department of Agricultural Entomology, College of Agriculture, University of Agricultural Sciences, Raichur, India.
[3]Department of Seed Science and Technology, College of Agriculture, University of Agricultural Sciences, Raichur - 584 101, Karnataka, India.

Authors' contributions

This work was carried out in collaboration among all authors. Author PSY conducted the study, performed the statistical analysis, wrote the protocol and wrote the first draft of the manuscript. Author SH designed the study, corrected the protocol. Author UN managed the analyses of the study. Author KTR managed the literature searches. Author AGS managed the literature searches. Author SRD managed the literature searches. All authors read and approved the final manuscript.

Article Information

DOI: 10.9734/IRJPAC/2020/v21i330159
Editor(s):
(1) Wolfgang Linert, Vienna University of Technology Getreidemarkt, Austria.
Reviewers:
(1) Ekane Peter Etape, University of Buea, Cameroon.
(2) Kevin C. Cannon, Penn State Abington College, USA.
(3) Ageng Trisna Surya Pradana Putra, Sultan Maulana Hasanuddin State Islamic University, Indonesia.
Complete Peer review History: http://www.sdiarticle4.com/review-history/55386

Original Research Article

Received 09 January 2020
Accepted 14 March 2020
Published 24 March 2020

ABSTRACT

The present work was aimed to study the synthesis of silver nanoparticles (Ag NPs) using Tri-Sodium Citrate (TSC), stability study of synthesized Ag NPs and their characterization. Synthesis of Ag NPs has been carried out by maintaining different conditions such as TSC concentration (0.50, 1.00 and 1.50%), $AgNO_3$ concentration (0.50, 1.00 and 1.50 mM) and stirring time (10, 15 and 20 min). The stability study of synthesized Ag NPs conducted for 30 days without adding any stabilizing agents. The characterization of synthesized Ag NPs was carried out for different parameters like particle size and zeta potential using particle size analyzer, absorbance peak by UV-Visible

**Corresponding author: E-mail: premsanthi.yerragopu@gmail.com;*

spectrophotometer, morphology by Scanning Electron Microscope (SEM), crystallinity by X-Ray Diffractometer (XRD) and material structural characteristics by Atomic Force Microscope (AFM). The stable chemically synthesized Ag NPs were obtained at C_{20} ($AgNO_3$ concentration of 1.5 mM, TSC 1.5% and stirring time 20 min) (desirability 99.97%), with average particle size of 22.14 nm and average absorbance peak of 449.85 nm.

Keywords: Absorbance peak; characterization; tri-sodium citrate; particle size; silver nanoparticles and stability study.

1. INTRODUCTION

Nanoscience and nanotechnology are the study and application of extremely small things and can be used across all the other science fields, such as chemistry, biology, physics, materials science and engineering. Nanotechnology is the study of phenomena and manipulation of materials at atomic, molecular and macromolecular scale. It is a rapidly growing field with its wide application in science and technology for manufacturing of new materials at nanoscale level [1]. It includes the synthesis, characterization, exploration and utilization of nanostructured materials. The nanostructured materials are very interesting both for scientific reasons and practical applications [2]. Despite the existence of numerous metals in nature, only a few of them such as gold, silver, palladium and platinum are synthesized extensively in nanostructured form [3]. Among the above mentioned metals, silver nanoparticles (Ag NPs) have attracted much attention due to their unique physical, chemical and biological properties compared to bulk silver for utilizing in various applications including pharmaceutics, agriculture, water detoxification, air filtration, food industries, textile industries and as a catalyst in oxidization reactions [4].

However, chemical method of synthesis is often used, due to its ease of production [5]. The very common approach for synthesis of Ag NPs by chemical reduction using organic and inorganic reducing agents. The selection of an suitable reducing agent is a important factor, as the size, shape and particle size distribution mostly depend on the nature of the reducing agent. The most popular synthesis of Ag NPs is chemical reduction of silver salts by Tri-Sodium Citrate (TSC) [6]. TSC act as both reducing and coordinating agent. Free electron pairs in carbonyl groups can stabilize nanoparticles electrostatically and act as a coordinating agent in compounds with metallic atoms that have free orbitals. The main advantage of the chemical reduction method using TSC is the possibility of further functionalization (citrate ions can be easily exchanged with other compounds due to weak interaction of citrate molecules with metal surfaces) [7]. The preparation is simple, but great care must be exercised. However, solution temperature, concentrations of metal salt, reducing agent and reaction time influence the particle size [6]. However, the lack of particle stability of Ag NPs has prevented the silver from wider applications [8].

Thus, the aim of this study was to synthesize silver nanoparticles using tri-sodium citrate and to conduct stability study and characterization of synthesized silver nanoparticles using various characterization instruments.

2. MATERIALS AND METHODS

2.1 Chemical Synthesis of Ag NPs Using Tri-sodium Citrate

The chemical synthesis of Ag NPs was carried out using the materials such as Tri-Sodium Citrate, Silver Nitrate (Ag NO_3) and the procedure was described below.

Hundred millilitres of (0.50, 1.00 and 1.50 mM) $AgNO_3$ solution was heated at 90°C for 5 min using water bath. To this 12.5 mL of the prepared TSC solution (0.50, 1.00 and 1.50%) was added drop by drop while continuously stirring. The reduction process begins with the colour change from transparent to pale yellow, which showed the formation of Ag NPs. The nanoparticle solution was stirred (10, 15 and 20 min) on a magnetic stirrer at 90°C and stored in refrigerator (8±1°C) for further stability study [9].

The treatment combinations for chemical synthesis of Ag NPs is given Table 1. Figs. 1 and 2 depicts the process flow chart for chemical synthesis of Ag NPs using TSC.

2.2 Stability Study of Chemically Synthesized Ag NPs

The stability study of chemically synthesized Ag NPs was conducted using twenty

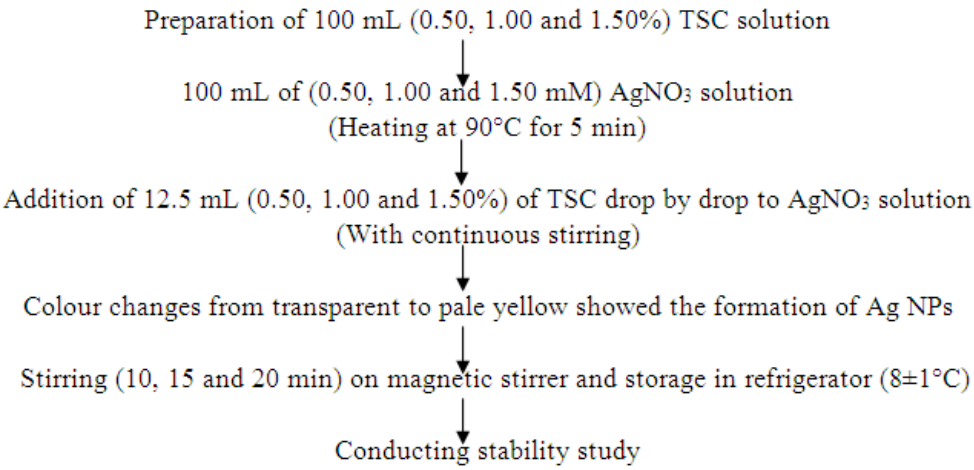

Fig. 1. Process flow chart for chemical synthesis of Ag NPs using TSC

Fig. 2. Process flow chart for chemical synthesis of Ag NPs using TSC

Different samples. The samples were stored in refrigerated condition (8±1°C) during the stability study and observed with particle size analyzer for particle size and UV-Visible spectrophotometer for absorbance peak for 30 days at an interval of 12 h.

2.3 Optimization of Treatment Combinations for Chemically Synthesized Ag Nps

Twenty experiments with three replications were performed in a randomized order. A second order quadratic polynomial model was used to fit the experimental data, to develop mathematical model and predict experimental data using Design Expert software (Version 7.0.0).

2.4 Characterization of Ag NPs

The characterization of synthesized Ag NPs was carried out for different parameters like particle size, zeta potential, absorbance peak, morphology, crystallinity and material structural characteristics. The optimized treatment combination obtained during the stability study was taken for further characterization with the following instruments.

2.5 Particle Size of Ag NPs Using Particle Size Analyzer

The particle size analyzer performs size measurements using a process called Dynamic Light Scattering (DLS). The principle of DLS is that fine particles and molecules are in constant random thermal motion, called Brownian motion, which diffuse at a speed related to their size, smaller particles diffuse faster than larger particles [10]. The average particle diameter (nm) was recorded from intensity graph.

2.6 Zeta Potential of Ag Nps Using Particle Size Analyzer

Zeta potential is a measure of the effective electric charge on the nanoparticle surface. The magnitude of the zeta potential provides information about particle stability, with values greater than +30 mV or less than -30 mV have high degrees of stability due to a larger electrostatic repulsion between particles [11]. Dispersions with a low zeta potential will eventually aggregate due to Vander Waal inter-particle attractions. A laser passes through the cell and as particles move through the laser beam the intensity of scattered light fluctuates at a rate proportional to the particle speed. Particle speed at multiple voltages is measured and used to calculate the zeta potential. The average zeta potential was recorded from the intensity graph.

2.7 Absorbance Peak of Ag NPs Using UV-visible Spectrophotometer

Absorbance peak of synthesized Ag NPs was measured using UV-Visible spectrophotometer. It works on the principle of Beer-Lambert law. This law states that whenever a beam of monochromatic light is passed through a solution with an absorbing substance, the decreasing rate of the radiation intensity along with the thickness of the absorbing solution is proportional to concentration of solution and incident radiation. From the Beer-Lambert law, it was determined that greater the number of molecules that were capable of absorbing light at a certain wavelength, greater the extent of the absorption of light. The wavelength that corresponds to the highest absorption is usually referred to as λ_{max}. The resulting spectrum was presented as a graph of absorbance (A) versus wavelength (λ). For Ag NPs the absorbance peak (λ_{max}) ranges from 380 to 450 nm [12]. The sample was prepared by diluting 1 mL of Ag NPs into 2 mL of distilled water and measuring the UV-Visible spectrum of solutions [13].

2.8 Surface Morphology of Ag NPs Using Scanning Electron Microscope

Surface morphology of synthesized Ag NPs was measured using Scanning Electron Microscope (SEM). SEM is a powerful magnification tool that utilizes focused beams of electrons to obtain information. It works on the principle that when the accelerated primary electrons strike the sample in vacuum chamber, it produces secondary electrons. These secondary electrons are collected by a positively charged electron detector which in turn gives a 3D image of the sample using the software and also backscattered electrons are higher energy electrons that are elastically backscattered by the atoms of the sample. Atoms with higher atomic numbers backscatter more efficiently and therefore this detector can give compositional information about the sample [14]. The magnification (1 to 500 kX) and focusing was carried out to get clear surface morphology of samples at the accelerating voltage range from 1 to 30 kV with working distance of the sample at 10 mm (8 to 25 mm) [15].

2.9 Phase Identification of Ag NPs Using X-Ray Diffractometer

Phase identification of synthesized Ag NPs was measured using X-Ray Diffractometer (XRD). XRD is a unique method in determination of crystallinity of a compound. It is based on constructive interference of monochromatic X-Rays and a crystalline sample. The X-Rays are generated by a cathode ray tube, filtered to produce monochromatic radiation and directed towards the sample. The interaction of the incident rays with the sample produces constructive interference, when conditions satisfy Bragg's law [16]. Synthesized Ag NPs (1 g) were uniformly spread on glass sample holder and placed in scanning chamber. The scan speed and step size were set by using ICDD PDF_2 software (Version V6.7) of 0.30º/min and 0.001 s, respectively and were fixed [17]. The XRD pattern was recorded for phase identification of Ag NPs.

2.10 Surface Imaging of Ag NPs Using Atomic Force Microscope

Surface imaging of synthesized Ag NPs was measured using Atomic Force Microscope (AFM). Atomic force microscope provides a 3D profile of the nanoparticles surface by measuring forces between a sharp probe (< 10 nm) and surface at very short distance (0.20 to 10 nm probe sample separation). The amount of force between the probe and sample is dependent on the spring constant, stiffness of the cantilever and the distance between the probe and the sample surface. This force can be described using Hooke's law [18]. Silver nanoparticle solution was placed on glass slide in a thin layer and dried in a hot air oven at 60°C for 10 min [19]. Glass slide containing sample was kept on the sample chamber by adjusting the cantilever of AFM. Laser beam was focused on the cantilever tip and glass slide to obtain 3D, 2D images, image profile and roughness coefficient values for individual samples.

3. RESULTS AND DISCUSSION

3.1 Chemical Synthesis of Ag NPs Using Tri-sodium Citrate

The Ag NPs were prepared by chemical reduction method using tri-sodium citrate (TSC). For this, TSC solution was added drop by drop to $AgNO_3$ solution after reaching to 90°C, resulting in a colour change and the mixture changed from transparent to pale yellow indicating the formation of Ag NPs. During the synthesis process, the reductant ($C_6H_5O_7Na_3$) directly reduced Ag^+ ions to generate metallic Ag^o atoms. The produced Ag^o atoms then acted as nucleation cites and catalysed the reduction of remaining metal ions present in the solution. The coalescence of atoms led to formation of metal clusters, which were normally stabilized by ligands, surfactants or polymers by using TSC as reducing agent [5]. The colour changed from light yellow to yellow and then greenish. These changes showed the formation of Ag NPs. The colour of metal nanoparticles based on the shape and size of the nanoparticles and the dielectric constant of the surrounding medium. A visible change in colour was observed using 1% TSC from transparent to yellowish brown [6].

3.2 Stability Study of Chemically Synthesized Ag NPs

From Table 1, it is observed that C_{20} ($AgNO_3$ concentration of 1.5 mM, TSC 1.5% and stirring time 20 min) was the best treatment combination with desirability of 99.97% in terms of stability among 20 different treatment combinations. During stability study, the size of nanoparticles was varied from 19.50 to 118.00 nm and absorbance peak varied from 393.50 to 476.00 nm. The effect of $AgNO_3$ concentration, TSC and stirring time on particle size and absorbance peak of chemically synthesized Ag NPs during stability study are given in Table 1.

From Table 1, it is noticed that the minimum particle size of 22.14 nm recorded at C_{20} ($AgNO_3$ concentration of 1.5 mM, TSC 1.5% and stirring time 20 min) and the maximum particle size of 86.96 nm at C_3 ($AgNO_3$ concentration of 0.16 mM, TSC 1.0% and stirring time 15 min). For particle size of chemically synthesized Ag NPs, F-value of the model observed was 9.79, R^2 value was 0.89 and it is significant. The minimum absorbance peak of 401.23 nm at C_6 ($AgNO_3$ concentration of 1.0 mM, TSC 0.16% and stirring time 15 min) and the maximum of 449.85 nm at C_{20} ($AgNO_3$ concentration of 1.5 mM, TSC 1.5% and stirring time 20 min) are also observed. For absorbance peak of chemically synthesized Ag NPs, F-value of the model observed was 11.04, R^2 value was 0.90 and it is significant. The interaction effects of $AgNO_3$ concentration, TSC and stirring time on particle size and absorbance peak are statistically significant ($p<0.01$) at 1% level.

Table 1. Treatment combinations and results (Particle size and absorbance peak) for synthesis of Ag NPs

Run	Treatment	$AgNO_3$ concentration (mM)	Tri-sodium citrate (%)	Stirring time (min)	Particle size (nm)	Absorbance peak (nm)
1	C_1	0.50	0.50	10.00	85.65	403.70
2	C_2	0.50	0.50	20.00	83.23	410.59
3	C_3	0.16	1.00	15.00	86.96	401.42
4	C_4	0.50	1.50	10.00	29.72	427.15
5	C_5	0.50	1.50	20.00	24.63	439.51
6	C_6	1.00	0.16	15.00	76.89	401.23
7	C_7	1.00	1.00	6.59	65.73	429.23
8	C_8	1.00	1.00	15.00	31.51	432.10
9	C_9	1.00	1.00	15.00	37.96	435.64
10	C_{10}	1.00	1.00	15.00	41.55	430.78
11	C_{11}	1.00	1.00	15.00	36.43	429.85
12	C_{12}	1.00	1.00	15.00	32.53	436.71
13	C_{13}	1.00	1.00	15.00	35.05	428.41
14	C_{14}	1.00	1.00	23.41	28.59	442.51
15	C_{15}	1.00	1.84	15.00	39.28	440.53
16	C_{16}	1.50	0.50	10.00	29.59	418.25
17	C_{17}	1.50	0.50	20.00	23.17	428.16
18	C_{18}	1.84	1.00	15.00	30.15	435.45
19	C_{19}	1.50	1.50	10.00	34.56	413.20
20	C_{20}	1.50	1.50	20.00	22.14	449.85

3.3 Effect of $AgNO_3$ Concentration, TSC and Stirring Time on Particle Size

The effect of $AgNO_3$ concentration and TSC on particle size is depicted in Fig. 3a. From the figure it is noticed that as the $AgNO_3$ concentration (0.5 to 1.5 mM) increased, there is a decrease in particle size from 34.01 to 32.96 nm. This might be due to increase in $AgNO_3$ concentration (0.2 to 0.4 mM), which lead to the formation of large number of tiny particles (8.6 nm) using $NaBH_4$ as reducing agent [20]. Whereas, increase in TSC (0.5 to 1.5%), decreased the particle size (89.10 to 29.82 nm). According to law of mass action, the reaction rate is proportional to reactant concentration. Therefore, the increase in TSC dihydrate concentration from 0.1 to 0.2%, increased the rate of reaction. As the reaction rate increased, the silver ions (Ag^+) were dissolved faster, thus having less possibility for particle size growth (37.24 to 43.04 nm) [5].

Fig. 3b depicts the effect of $AgNO_3$ concentration and stirring time on particle size. From the figure it is observed that as the $AgNO_3$ concentration increased from 0.5 to 1.5 mM, decreased the particle size from 62.78 to 34.94 nm. This might be due to increase in $AgNO_3$ concentration (0.2 to 0.4 mM), which lead to the formation of large number of tiny particles [20]. Whereas, increase in stirring time (10 to 20 min), decreased particle size (52.60 to 19.10 nm). This might be due to shift in SPR peak. Contact time is one of the parameters that controls the size of Ag NPs because of blue shift in adsorption peaks. It could be inferred that, at the early stage the SPR band was broadened because of the slow conversion of silver ion (Ag^+) to zerovalent silver (Ag°) nanoparticles. However, further increase in the contact time led to effective decrease in nanoparticle size (1 to 5 nm) using $NaBH_4$ as reducing agent [21].

From Fig. 3c, the effect of TSC and stirring time on particle size is observed. With the increase in TSC from 0.5 to 1.5%, the particle size decreased from 49.51 to 21.87 nm. This might be due to increase in TSC concentration which increased the rate of reaction and thus in turn decreased the particle size from 50 to 5 nm [13]. Whereas, the increase in stirring time from 10 to 20 min, decreased the particle size from 60.35 to 37.04 nm. This might be due to the shift in SPR which resulted in reduction of particle size [21].

The variation in particle size might be due to difference in reducing agent (TSC), $AgNO_3$ concentration, TSC concentration and stirring time.

3.4 Effect of $AgNO_3$ Concentration, TSC and Stirring Time on Absorbance Peak

Fig. 4a. depicts the effect of $AgNO_3$ concentration, TSC on absorbance peak. From the figure it is noticed that as the $AgNO_3$ concentration (0.5 to 1.5 mM) increased, the absorbance peak increased (402.37 to 423.86 nm). This might be due to increase in $AgNO_3$ concentration which increased the rate at which the SPR was attained. Ag NPs formed within the wavelength range of 400.00 to 490.00 nm which showed the formation of Ag° nanoparticles [21]. The increase in TSC (0.5 to 1.5%), increased the absorbance peak (431.09 to 434.72 nm). This might be due to the fact that absorbance peak increases with increased citrate concentration and attained a plateau at higher citrate ion concentration. The higher the concentration, complexation of the Ag ions with citrate ions with maximum absorbance of 420 nm was achieved [22].

The effect of $AgNO_3$ concentration and stirring time on absorbance peak is shown in Fig. 4b. It is observed that increase in $AgNO_3$ concentration from 0.5 to 1.5 mM, increases absorbance peak from 419.00 to 424.73 nm. This might be due to increase in $AgNO_3$ concentration. This in turn increased the rate at which the SPR was attained resulting in increase of absorbance peak [21]. On the other hand, the increase in stirring time from 10 to 20 min, increased absorbance peak (425.08 to 444.46 nm). This might be due to increased contact time which enhanced the absorbance peak due to excellent SPR band formation as large amount of Ag^+ has been converted to Ag° [21].

Fig. 4c depicts the effect of TSC and stirring time on absorbance peak. From the figure it is observed that as the TSC increased from 0.5 to 1.5%, the absorbance peak increased from 416.86 to 428.60 nm. This was probably due to complete complexation of the Ag ions with increase in citrate ions concentration [22]. On the other hand, the increase in stirring time from 10 to 20 min has increased the absorbance peak from 421.71 to 449.56 nm which was due to increasing the contact time and thereby the absorbance peak increased because large amount of Ag^+ has been converted to Ag° [21].

3.5 Characterization of Ag NPs

Optimized sample obtained during the stability study of chemically synthesized Ag NPs were characterized by using various instruments *viz*., Particle size analyzer, UV-Visible spectrophotometer, Scanning Electron Microscope (SEM), X-Ray Diffractometer (XRD) and Atomic Force Microscope (AFM).

3.6 Particle Size of Chemically Synthesized Ag NPs

The average diameter of chemically synthesized Ag NPs using tri-sodium citrate is found to be 31.95 nm from the intensity distribution analysis using Particle size analyzer. Fig. 5 shows the DLS pattern of the suspension of chemically synthesized Ag NPs (31.95 nm) using TSC.

Ag NPs size ranged from 7 to 20 nm with mean diameter of 9 nm with 0.02% of TSC as reducing agent and 1 mM $AgNO_3$ [23]. The variation in particle size might be due to the difference in $AgNO_3$ (0.5 to 1.5 mM) and TSC concentration (1.5%). The diameter of the Ag NPs ranged between 18 and 30 nm using tannic acid as reducing agent [24]. The variation might be due to change in reducing agent.

3.7 Zeta Potential of Chemically Synthesized Ag NPs

The zeta potential value of chemically synthesized Ag NPs using TSC is observed to be -26.00 mV and its conductivity is 0.262. Hence, the quality of chemically synthesized Ag NPs is found to be good and Fig. 6 depicts the zeta potential distribution.

The electrostatic stabilization of various synthesized Ag NPs was estimated by measuring their zeta potential values using sodium borohydride ($NaBH_4$) as reducing agent. The zeta potential value was found to be in the range from -26.80 to -53.10 mV [25].

The synthesis of nanoparticles using $NaBH_4$, the zeta potential values was found to be -53.18 mV [26]. They reported that, the presence of strong electric charges on the particle surfaces hinder the agglomeration and kept all the particles away from each other. This variation in zeta potential values might be due to difference in reducing agent (TSC).

3.8 Absorbance Peak of Chemically Synthesized Ag NPs

The UV-Visible absorption spectrum of chemically synthesized Ag NPs exhibited

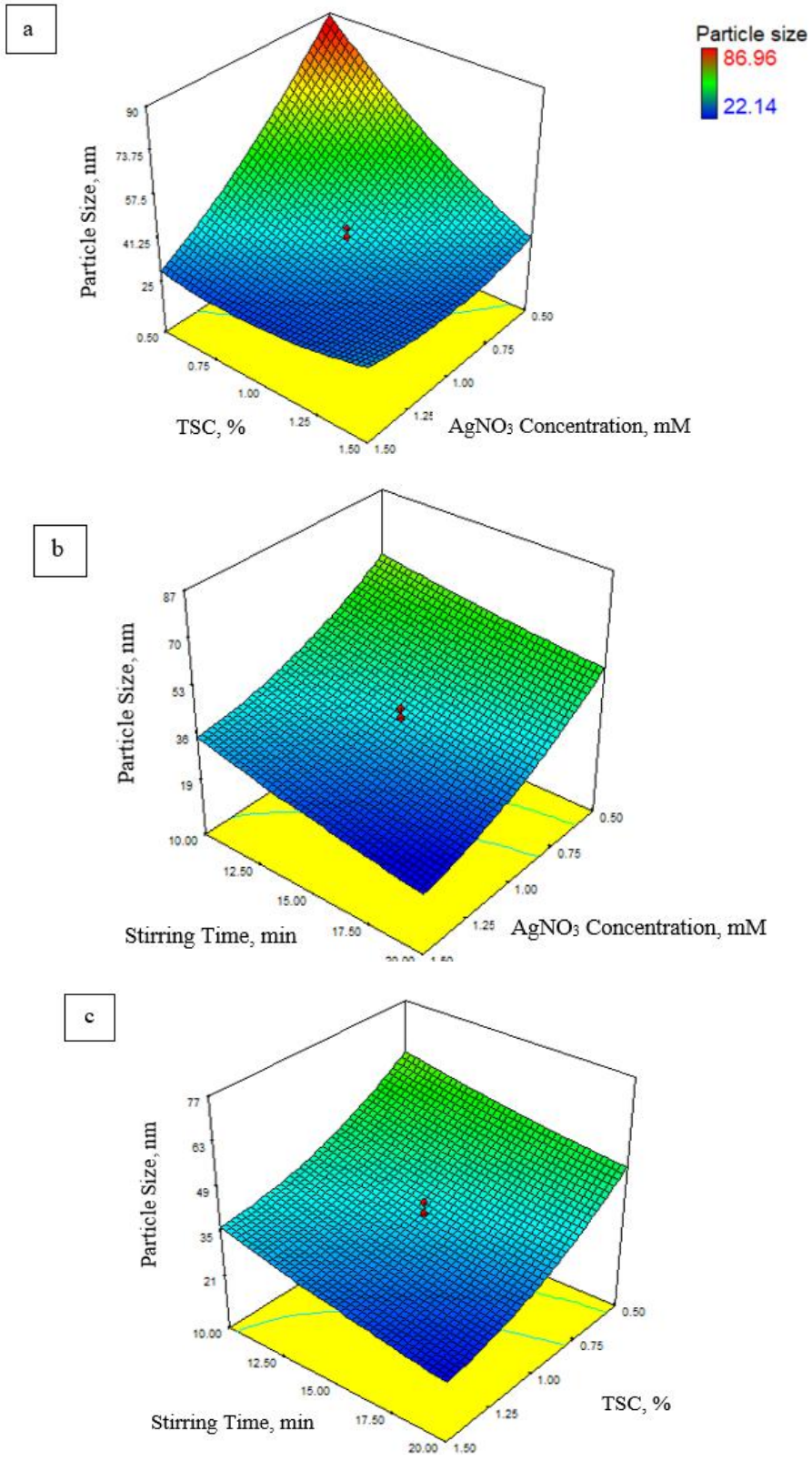

Fig. 3. Response surface plots of particle size for chemically synthesized silver nanoparticles as a function of (a) $AgNO_3$ concentration and TSC (b) $AgNO_3$ concentration and stirring time (c) TSC and stirring time

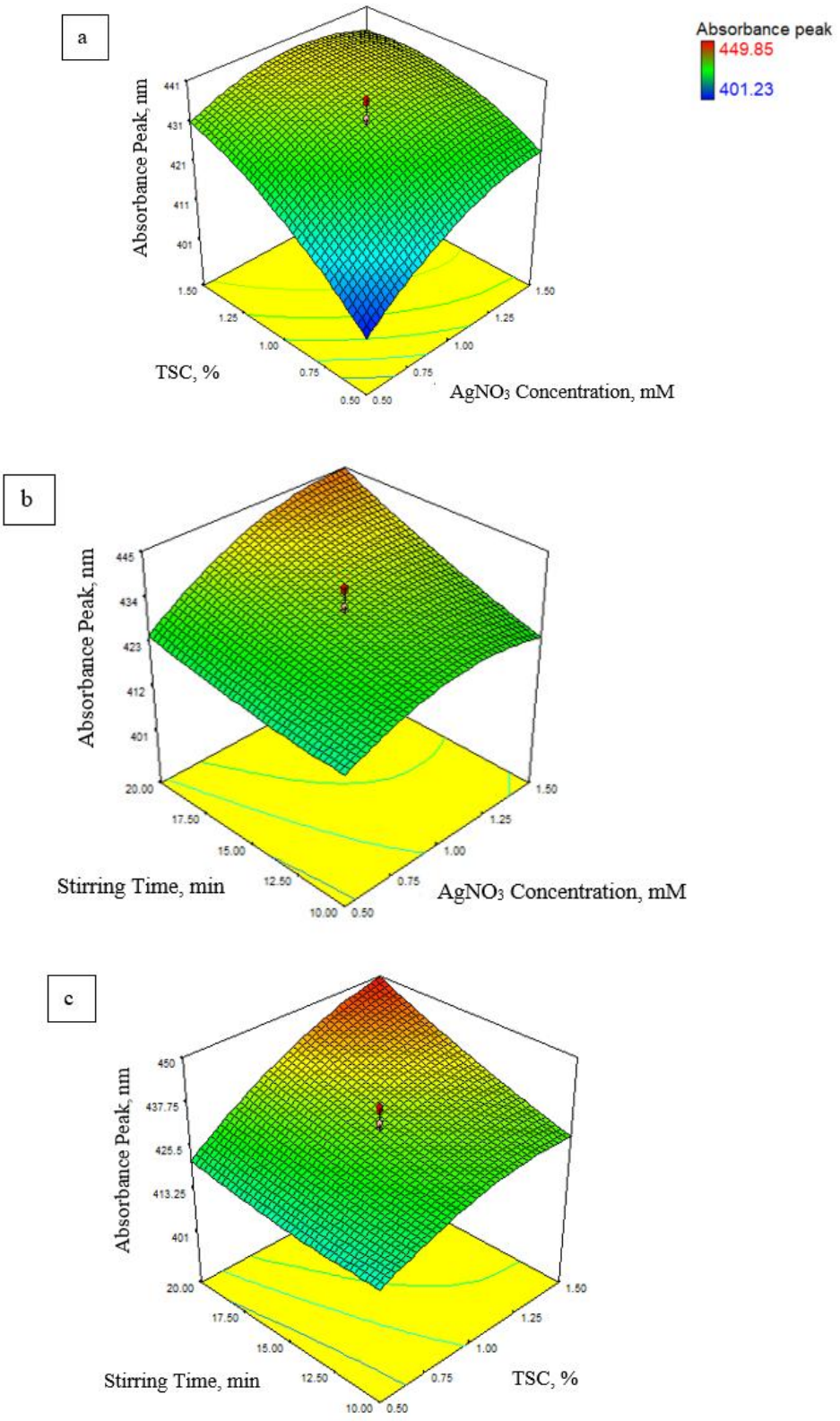

Fig. 4. Response surface plots of absorbance peak for chemically synthesized silver nanoparticles as a function of (a) $AgNO_3$ concentration and TSC (b) $AgNO_3$ concentration and Stirring time (c) TSC and stirring time

characteristic SPR band centered at wavelength of 434.65 nm and absorbance of 0.49 (Fig. 7).

The absorption peak of Ag NPs was 450 nm. UV-Visible absorption spectrum results confirmed the formation of Ag NPs by chemical reduction method ($AgNO_3$ reduced by TSC $C_6H_5O_7Na_3$) with absorption peak at 450 nm [6]. The UV-Visible absorption band centered at 420 nm was the characteristic absorption of Ag NPs using TSC [22].

3.9 Surface Morphology of Chemically Synthesized Ag NPs

SEM image of chemically synthesized Ag NPs is observed to be spherical in shape with magnification of 7.42 kX at the accelerating voltage of 10.00 kV with working distance of 10.00 mm as shown in Fig. 8.

Using TSC it was reported that SEM image of the Ag NPs synthesized indicated well dispersed particles that were more or less spherical [6]. The morphology of synthesized Ag NPs using SEM with sodium citrate as reducing agent (spherical) observed similar results [22].

3.10 Phase Identification of Chemically Synthesized Ag NPs

XRD pattern of chemically synthesized showed five distinct diffraction peaks at 31.17º, 46.02º, 48.45º, 54.60º and 57.28º that are corresponding to (111), (200), (220), (222) and (311) reflection planes, respectively. The highest peak is observed at 31.17º (111) reflection. The XRD study confirmed that, the nanoparticles are FCC in nature and intensity of the peaks reflected high degree of crystallinity of Ag NPs. It confirmed that the main composition of the nanoparticles is silver. The crystalline nature of Ag NPs is

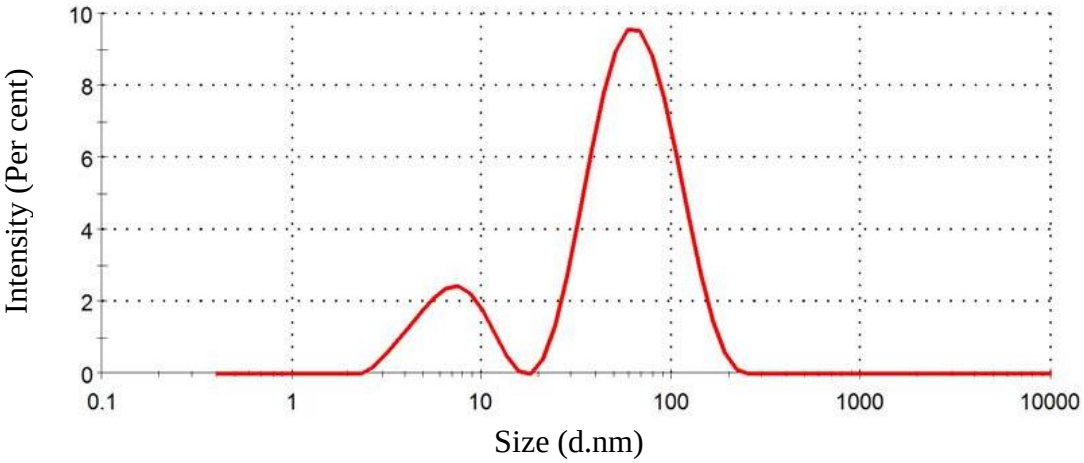

Fig. 5. Average particle size of chemically synthesized Ag NPs

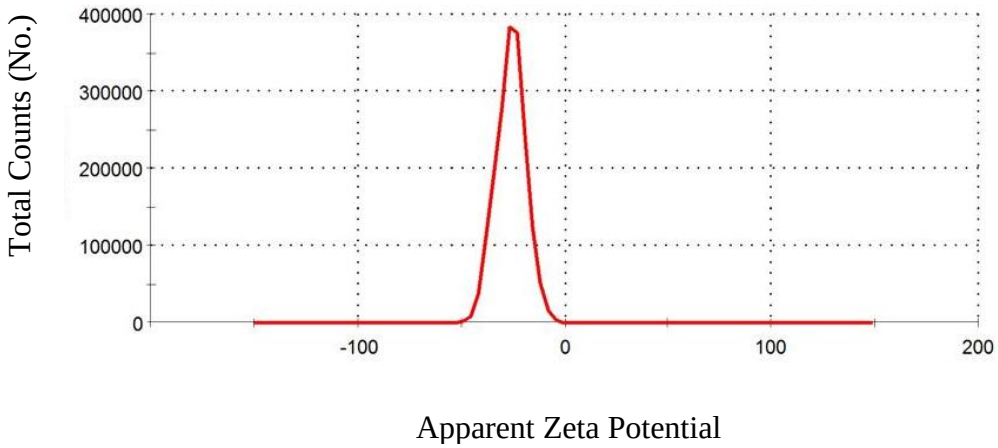

Fig. 6. Zeta potential distribution of chemically synthesized Ag NPs

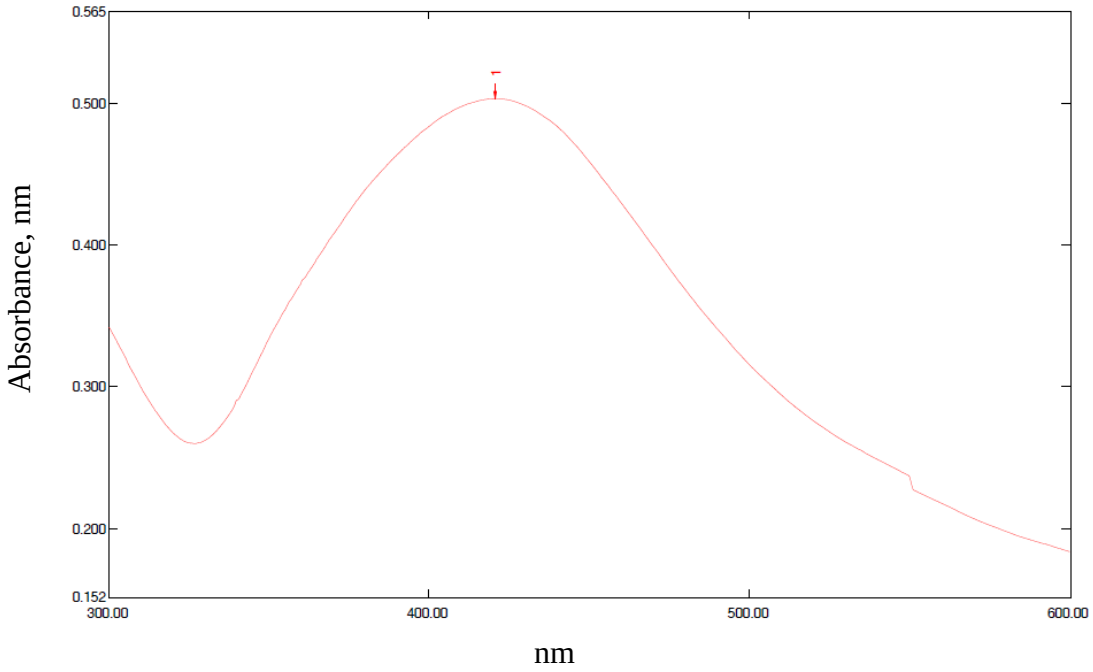

Fig. 7. Absorbance peak of chemically synthesized Ag NPs

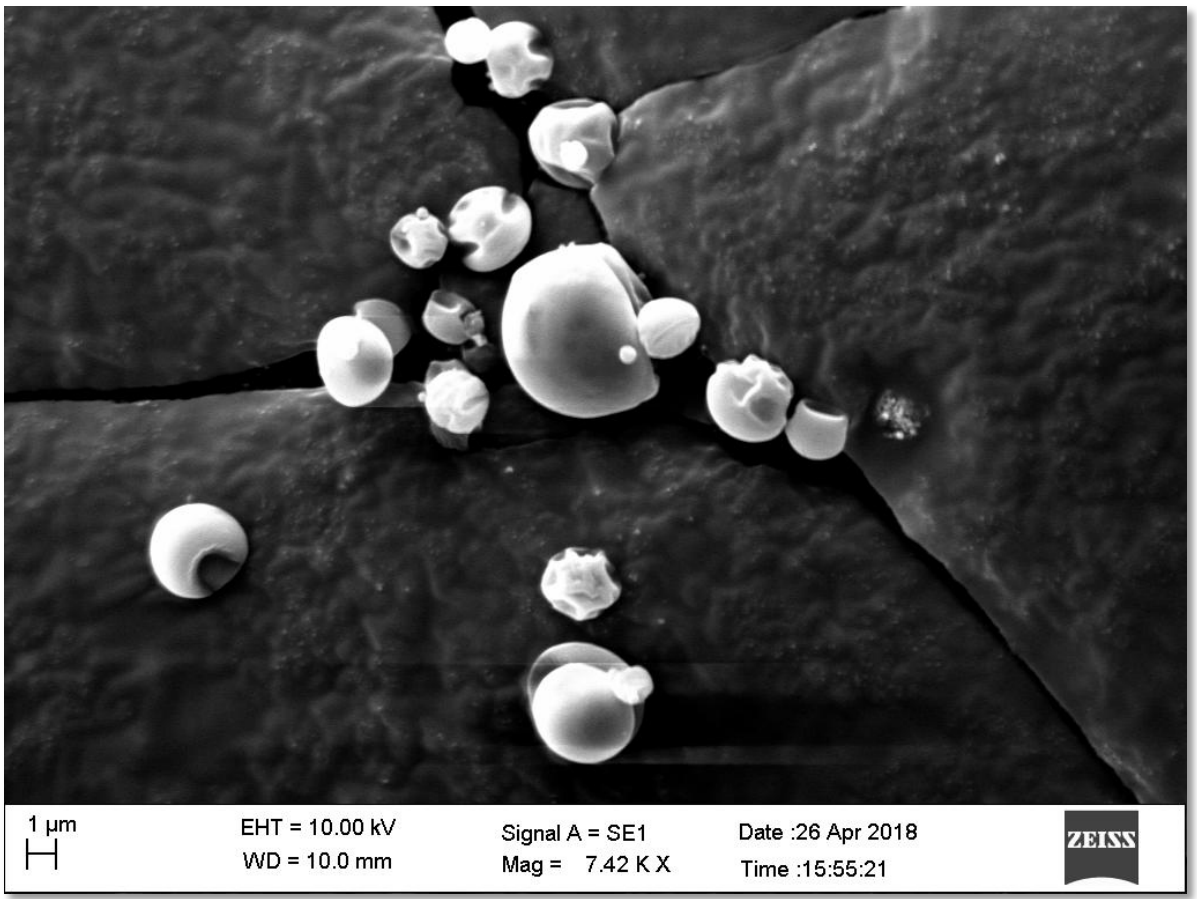

Fig. 8. SEM image of chemically synthesized Ag NPs

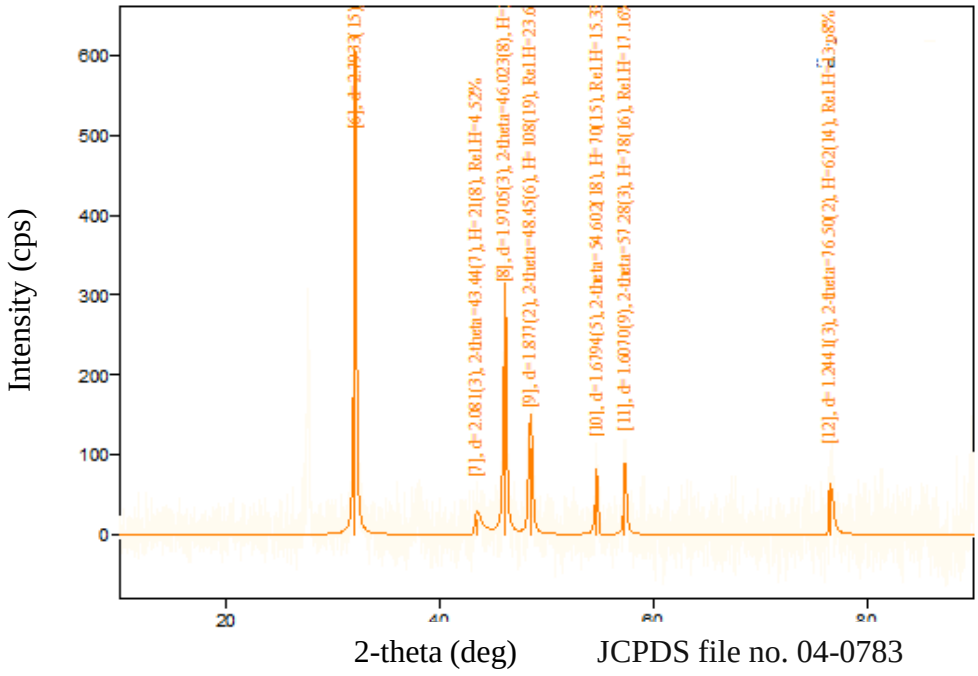

Fig. 9. XRD analysis of chemically synthesized Ag NPs

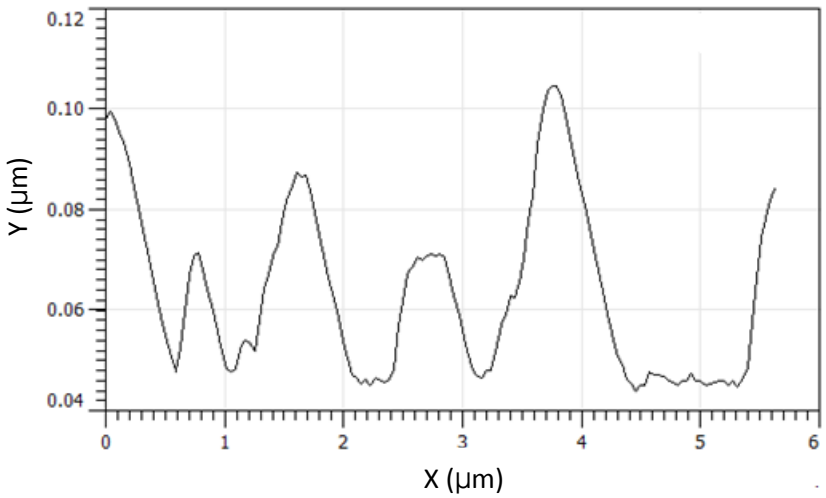

Fig. 10. AFM profile of chemically synthesized Ag NPs

confirmed from the XRD analysis of chemically synthesized Ag NPs using TSC as shown in Fig. 9.

The XRD pattern of synthesized Ag NPs using TSC, obtained from Bragg's reflection index (111), (220) and (311) which corresponds to the FCC structure and also shows that synthesized Ag NPs were crystalline. However, it can also be observed that the peaks are substantially broadened, indicating that the material is composed of very little quantity of silver crystals [5]. The synthesized Ag NPs using TSC showed diffraction peaks at 2θ values of 38.2°, 44.4° and 64.6° which can be indexed to (111), (200) and (220) planes of pure silver. All the peaks in XRD pattern can be readily indexed to a FCC structure of silver [27].

3.11 Surface Imaging of Chemically Synthesized Ag NPs

For chemically synthesized Ag NPs, height and width of the arbitrarily selected particles are 210 and 40 nm, whereas roughness average and root mean square roughness are recorded as

10.8535 and 15.3217 nm, respectively. The AFM profile of chemically synthesized Ag NPs sample which indicates the height (Y axis) and width (X axis) of the Ag NPs is depicted in Fig. 10.

Larger roughness value was obtained due to the rough surface area of the Ag NPs. Some nanoparticles were agglomerated, this might be due to the deposition of the Ag NPs on the surface tending to form cluster together during the analysis [28]. AFM micrographs with a scanning area of 3 × 3 µm obtained from silver thin films was having root mean square surface roughness (Rq) value of 1.715 [18]. The variation in the root mean square surface roughness might be due to the difference in the reducing agent (TSC) considered for the present study.

4. CONCLUSIONS

Chemical synthesis of Ag NPs was carried out by using tri-sodium citrate as reducing agent shows a colour change and the mixture changes from transparent to pale yellow indicating the formation of Ag NPs. The stability study was conducted for 20 different samples to determine the stability of Ag NPs, observed that C_{20} ($AgNO_3$ concentration of 1.5 mM, TSC 1.5% and stirring time 20 min) was the best treatment combination (desirability 99.97%), with average particle size of 22.14 nm and average absorbance peak of 449.85 nm. Characterization of synthesized Ag NPs was analysed using particle size analyzer (Partcle size 31.95 nm and Zeta potential -26.00 mV), UV-Visible spectrophotometer (Absorbance peak 434.65 nm and Absorbance 0.49), SEM (Morphology is spherical), XRD (FCC in nature) and AFM (Height 210 nm and Width 40 nm).

ACKNOWLEDGEMENT

The authors gratefully acknowledge the Senior Research Fellowship (SRF) sponsored by Indian Council of Agricultural Research (ICAR), Govt. of India.

COMPETING INTERESTS

Authors have declared that no competing interests exist.

REFERENCES

1. Yang Y, Jin P, Zhang X, Ravichandran N, Ying H, Yu C, Ying H, Xu Y, Yin J, Wang K. New epigallocatechin gallate (EGCG) nanocomplexes co-assembled with 3-mercapto-1-hexanol and β-lactoglobulin for improvement of antitumor activity. Journal of Biomedicine and Nanotechnology. 2017; 13(3):805-814.
2. Gan L, Zhang S, Zhang Y, He S, Tian Y. Biosynthesis, characterization and antimicrobial activity of silver nanoparticles by a Halotolerant *Bacillus endophyticus* SCU-L. Preparative Biochemistry and Biotechnology. 2018;7(2):582-588.
3. Korshed P, Li L, Ngo DT, Wang T. Effect of storage conditions on the long-term stability of bactericidal effects for laser generated silver nanoparticles. Nanomaterials. 2018;8(4):218-230.
4. Albrecht MA, Evans CW, Raston CL. Green chemistry and the health implications of nanoparticles. Green Chemistry. 2006;8 (5):417-432.
5. Pathak KCS, Mishra DD, Agarwala V, Mandal MK. Optical properties of ZnS nanoparticles prepared by high energy ball milling. Materials Science in Semiconductor Processing. 2013;16(2): 525-529.
6. Suriati G, Mariatti M, Azizan A. Synthesis of silver nanoparticles by chemical reduction method: Effect of reducing agent and surfactant concentration. International Journal of Automotive and Mechanical Engineering. 2014;10(1):1920-1927.
7. Udapudi B, Naik PK, Savadatti ST, Sharma R, Balgi S. Synthesis and characterization of silver nanoparticles. International Journal of Pharmacy and Biological Science. 2012;2(3):10-14.
8. Soliwoda KT, Tomaszewska E, Socha E, Krzyczmonik P, Ignaczak A, Orlowski P, Krzyzowska M, Celichowski G, Grobelny J. The role of tannic acid and sodium citrate in the synthesis of silver nanoparticles. Journal of Nanoparticle Research. 2017;19 (8):1-15.
9. Chowdhury S, Yusof F, Faruck MO, Sulaiman N. Process optimization of silver nanoparticle synthesis using response surface methodology. Procedia Engineering. 2016;142(2):992-999.
10. Das D, Yang Y, Brien OJS, Breznan D, Nimesh S, Bernatchez S, Hill M, Sayari A, Vincent R, Kumarathasan P. Synthesis and physicochemical characterization of mesoporous SiO_2 nanoparticles. Journal of Nanomaterials. 2014;62(6):11-12.
11. Kremer F. Fundamentals of interface and colloid science. International Journal of Research in Physical Chemistry and Chemical Physics. 1997;199(1):121-127.

12. Kadukova JS, Velgosova O, Vosatka M, Lukavsky J, Dodd J, Willner J, Fornalczyk, A. Control over the biological synthesis of Ag nanoparticles by selection of the specific algal species. Archives of Metallurgy and Materials. 2017;62(3):1439-1442.
13. Habibi B, Hadilou H, Mollaer S, Yazdinezhad A. Green synthesis of silver nanoparticles using the aqueous extract of *Prangos ferulaceae* leaves. International Journal of Nano Dimensions. 2017;8(2): 132-141.
14. Haq IU, Akhtar K, Malik A. Effect of experimental variables on the extraction of silica from the rice husk ash. Journal of the Chemical Society of Pakistan. 2014;36 (3):382-387.
15. Kim SK, Sohn EY, Lee IJ. Starch properties of native foxtail millet (*Setaria italica Beauv*). Journal of Crop Science and Biotechnology. 2009;12(1):59-62.
16. Halawani EM. Rapid biosynthesis method and characterization of silver nanoparticles using *Zizyphus spina christi* leaf extract and their antibacterial efficacy in therapeutic application. Journal of Biomaterials and Nanobiotechnology. 2017;8(1):22-35.
17. Djangang CN, Mlowe S, Njopwouo D, Revaprasadu N. One-step synthesis of silica nanoparticles by thermolysis of rice husk ash using nontoxic chemicals ethanol and polyethylene glycol. Journal of Applicable Chemistry. 2015;4(4):1218-1226.
18. Hong R, Ji J, Tao C, Zhang D, Zhang D. Fabrication of Au/graphene oxide/Ag sandwich structure thin film and its tunable energetics and tailorable optical properties. Material Sciences. 2017;4(1):223-230.
19. Rafiq Z, Nazir R, Shahwar DE, Shah MR, Ali S. Utilization of magnesium and zinc oxide nanoadsorbents as potential materials for treatment of copper electroplating industry wastewater. Journal of Environmental Chemical Engineering. 2014;2(1):642-651.
20. Sosa YD, Rabelero M, Trevino ME, Saade H, Lopez RG. High-yield synthesis of silver nanoparticles by precipitation in a high-aqueous phase content reverse microemulsion. Journal of Nanomaterials. 2010;3(1):1-6.
21. Dada AO, Folahan A, Adekola Oluyomi S. Adeyemi Oluwasesan M, Bello Adetunji C, Oluwaseun Oluwakemi J, Awakan, Grace FA. Exploring the effect of operational factors and characterization imperative to the synthesis of silver nanoparticles. Intech Open. 2018;2(5):165-184.
22. Zhou G, Wang W. Synthesis of silver nanoparticles and their antiproliferation against human lung cancer cells in vitro. Oriental Journal of Chemistry. 2012;28(2): 651-655.
23. Guzman MG, Dille J, Godet S. Synthesis of silver nanoparticles by chemical reduction method and their antibacterial activity. International Journal of Chemical and Biomolecular Engineering. 2008;2(3): 104-111.
24. Dadosh T. Synthesis of uniform silver nanoparticles with a controllable size. Materials Letters. 2009;63(7):2236-2238.
25. Agnihotri S, Mukherji S, Mukherji S. Size controlled silver nanoparticles synthesized over the range 5-100 nm using the same protocol and their antibacterial efficacy. Royal Society of Chemistry. 2014;4(2): 3974-3983.
26. Haider MJ, Mehdi MS. Study of morphology and zeta potential analyzer for the silver nanoparticles. International Journal of Scientific and Engineering Research. 2014;5(7):381-387.
27. Ho VTT, Thi ND. Synthesis of silver nanoparticles via chemical reduction and its anti-bacterial activities in wastewater of shrimp pond. International Journal of Engineering Research and Technology. 2016;5(6):1-5.
28. Alahmad A. Preparation and characterization of silver nanoparticles. International Journal of Chemtech Research. 2014;6(1):450-459.

Peer-review history:
The peer review history for this paper can be accessed here:
http://www.sdiarticle4.com/review-history/55386